Eur. J. Mineral.
2002, **14**, 127–133

Satterlyite, $(Fe,Mg)_{12}(PO_3OH)(PO_4)_5(OH,O)_6$: crystal structure and infrared absorption spectra

UWE KOLITSCH[1], MICHAEL ANDRUT and GERALD GIESTER

Institut für Mineralogie und Kristallographie, Geozentrum, Universität Wien, Althanstr. 14, A-1090 Wien, Austria
[1]e-mail: uwe.kolitsch@univie.ac.at

Abstract: The crystal structure of satterlyite from the Big Fish River area, Yukon Territory, Canada, $(Fe_{0.77}Mg_{0.23})_{12}(PO_3OH)(PO_4)_5(OH,O)_6$ (space group $P31m$, a = 11.355(1), c = 5.0394(5) Å, V = 562.71(9) Å^3, Z = 1), has been solved and refined using single-crystal intensity data (Mo $K\alpha$ X-radiation, CCD area detector, 2320 unique reflections with $F_o > 4\sigma(F_o)$, $R1$ = 2.15 %). The structure is based upon pairs of face-sharing, distorted $(Fe,Mg)O_6$ octahedra linked by edge-sharing to form double chains along [001]. Each double chain shares ligands with six other double chains to produce a three-dimensional network hosting three unique PO_4 tetrahedra which are corner-linked to the $(Fe,Mg)O_6$ octahedra. The two unique $(Fe,Mg)O_6$ octahedra are characterised by different occupancies; Fe:Mg ratios of the $M(1)$ and $M(2)$ sites are 0.838(2):0.162(2) and 0.706(2):0.294(2), respectively. Two H atoms are each bonded to common ligands of the two $(Fe,Mg)O_6$ octahedra. The third, strongly disordered H(3) atom is bonded to the apical O of the $P(1)O_4$ tetrahedron. The H(3) site and possibly both the other two H sites are only partially occupied, and only very weak hydrogen bonds exist. Satterlyite is isostructural with holtedahlite, $Mg_{12}(PO_3OH,CO_3)(PO_4)_5(OH,O)_6$. Unlike in natural holtedahlite, there is no carbonate-for-phosphate substitution in the satterlyite investigated, which was also confirmed by IR absorption powder spectra. A structural relationship exists with phosphoellenbergerite, $Mg_{14}(PO_4)_6(PO_3OH)_2(OH)_6$. Polarised IR spectra of oriented cut single crystals in the O-H stretching vibrational range revealed an asymmetric band at 3536 cm^{-1} (including a weak shoulder at ~3568 cm^{-1}) and an asymmetric band at ~3471 cm^{-1}. The number of hydroxyl vibrational bands and their positions are in accordance with the results of the structure refinement.

Key-words: satterlyite, crystal structure, crystal chemistry, infrared spectroscopy, holtedahlite.

Introduction

Satterlyite is a rare hydroxyl-bearing ferrous phosphate with the originally proposed simplified formula $(Fe^{2+},Mg)_2(PO_4)OH$. It has been first described by Mandarino *et al*. (1978) from the Big Fish River area, Yukon Territory, Canada, which represents the only occurrence known (Robertson, 1982; Robinson *et al*., 1992). At the type locality, the mineral is a rare constituent of epigenetic phosphatic nodules and forms divergent, columnar aggregates of crude, glassy crystals up to several centimetres in length. Crystallisation occurred at temperatures of about 180 – 200°C according to fluid inclusion studies (Robinson *et al*., 1992). Satterlyite was found to be trigonal, with the possible space groups $P\bar{3}1m$, $P31m$ and $P312$ (Mandarino *et al*., 1978). Some grains showed undulatory extinction and anomalously biaxial interference figures, with $2V_\alpha$ ranging between 10 and 20° (Mandarino *et al*., 1978). According to electron microprobe analyses, additional minor elements include Na, Mn, and traces of Si (Mandarino *et al*., 1978). The water content and a Fe^{2+}:Fe^{3+} ratio of 6.42:1.00 were determined by wet chemical analyses and the reported empirical formula was $(Fe^{2+}_{1.21}Mg_{0.36}Fe^{3+}_{0.19}H_{0.16}Na_{0.10}Mn_{0.04})_{\Sigma 2.06}P_{0.99}Si_{0.01}O_4(OH)$ (note the excess H in the cationic part of the formula). Mandarino *et al*. (1978) considered satterlyite dimorphous with (monoclinic) wolfeite which also occurs at the mentioned locality in Canada and forms a series with its Mn^{2+} analogue triploidite, $(Mn^{2+},Fe^{2+})_2(PO_4)OH$.

In a determination of the crystal structure of natural and synthetic crystals of the magnesium phosphate holtedahlite, $Mg_{12}(PO_3OH,CO_3)(PO_4)_5(OH,O)_6$ and $Mg_{12}(PO_3OH)(PO_4)_5(OH,O)_6$, respectively, Rømming & Raade (1989) stated that holtedahlite represents the Mg analogue of satterlyite, a conclusion based on an earlier solution of the crystal structure of satterlyite by Dr. Y. Le Page (R = 2.1 %, space group $P31m$). Unfortunately, the respective manuscript was never published (Y. Le Page, pers. comm., 1999). The aim of the present work was to determine the crystal structure of satterlyite, supplement the results with IR spectroscopic data, and compare the results with available data for holtedahlite. A comparison of these two structures was also of interest because in natural holtedahlite, one of three unique phosphate groups is partially replaced by carbonate groups (Rømming & Raade, 1989), a substitution mechanism which is also known from a very small number of other phosphates such as carbonate-bearing whitlockite,

0935-1221/02/0014-0127 $ 3.15
DOI: 10.1127/0935-1221/2002/0014-0127

$Ca_9(Mg,Fe^{2+})(PO_4)_6(PO_3OH,CO_3)$ (Frondel, 1949), carbonate-fluorapatite, $Ca_5(PO_4,CO_3)_3(F,OH)$ (Regnier *et al.*, 1994; Comodi & Liu, 2000), carbonate-bearing phosphoellenbergerite, $Mg_{12}(Mg,Fe,\square)_2(PO_4,PO_3OH,AsO_4)_6(PO_3OH,CO_3)_2(OH)_6$ (Raade *et al*., 1998), and possibly krasnovite, $Ba(Al,Mg)(PO_4,CO_3)(OH)_2 \cdot H_2O$ (Britvin *et al*., 1996; crystal structure is unknown, however). Infrared spectroscopy of satterlyite powder samples investigated earlier by Raade & Mladeck (1979) and Rømming & Raade (1989) gave no evidence of any carbonate contents.

Experimental

Crystal fragments were taken from a small satterlyite specimen from the Big Fish River area, Yukon Territory, Canada, from the collection of the first author. The monomineralic specimen consists of transparent, yellow-brown divergent columnar aggregates. Single-crystal studies show that the morphological elongation is along the *c*-axis. Semiquantitative energy-dispersive chemical analyses (JEOL JSM-6400, 20 kV acceleration voltage, LINK eXL10 software) were performed on carbon-coated fragments from the same large grain which provided the fragments for the subsequent structure determination. The analyses showed major Fe and P, minor Mg and very minor Mn (Fe:Mn *ca.* 15:1 – 10:1). Previous electron microprobe analyses of satterlyite from Yukon Territory revealed similar elemental ratios although with lower Mn contents (Mandarino *et al*., 1978). Optically, the fragments were uniaxial and showed normal interference colours.

A thermogravimetric analysis was done with a Mettler M3 microbalance on powdered handpicked satterlyite grains (sample weight 10.099 mg, heating rate 1 K/min, T = 900°C, flowing N_2 of 6.0 purity) in an attempt to determine the water content.

Infrared absorption measurements were carried out using a Bruker IFS 66v/S FTIR spectrometer equipped with a globar light source, a KBr beam splitter and a DTGS detector and liquid nitrogen-cooled MCT-detector. Spectra were averaged over 1024 scans. Phase correction mode of the interferogram was performed with a procedure after Mertz (Mertz, 1965; *cf*. Griffiths & de Haseth, 1986). Norton-Beer-weak mode was chosen as the apodisation function. The sample chamber of the Bruker IFS 66v/S was evacuated down to 200 Pa, thus minimising the influence of H_2O vapour and CO_2. The powdered sample was prepared by grinding 0.5 mg of substance and dispersing it into 450 mg of KBr. The mixture was subsequently pressed under vacuum to a transparent pellet 13 mm in diameter. The absorption measurements were carried out in the spectral range of 2000 to 400 cm^{-1} at a resolution of 2.0 cm^{-1}.

Polarised single-crystal spectra were recorded from 8 µm thick crystal plate, with the platy face accurately oriented perpendicular to the *a*-axis, in the spectral range 7500 to 1500 cm^{-1} at a resolution of 1 cm^{-1}. The spectra were recorded using a micro-focusing unit equipped with a KRS-5 polariser in the sample chamber of the spectrometer. An image mask with a diameter of 200 µm provided measuring spots smaller than the field of view. The single-crystal spectra were corrected for thickness and are displayed in the form of linear extinction coefficient as a function of wave number. After background correction, the band centre was determined with the program PeakFit (Jandel Scientific). Gaussian functions were used to describe the band shape.

Table 1. Crystal data, data collection information and refinement details for satterlyite.

Crystal data	
Formula	$(Fe_{0.77}Mg_{0.23})_{12}(PO_3OH)(PO_4)_5(OH,O)_6$
Space group	*P*31m
a, *c* (Å)	11.355(1), 5.0394(5)
V (Å^3), *Z*	562.71(9), 1
F(000), ρ_{calc} (g·cm^{-3})	613, 3.728
µ (mm^{-1})	6.58
Crystal dimensions (mm)	~0.18 x ~0.17 x ~0.11
Absorption correction	empirical*
Data collection and refinement	
Diffractometer	Nonius KappaCCD system
Temperature (K)	293
λ (Mo*K*α) (Å)	0.71073
Detector distance (mm)	28
Rotation axes	φ, ω
Rotation width (°)	1.5
Total no. of frames	451
Collect. time per frame (s)	35
$2\theta_{max}$ (°)	80.42
h, k, l ranges	-20 → 20, -17 → 17, -8 → 9
Total reflections measured	4311
Unique reflections	2357
*R*1(*F*), w*R*2(F^2)**	2.15 %, 4.88 %
'Observed' refls.	2320 [$F_o > 4\sigma(F_o)$]
Extinct. coefficient	0.0304(11)
No. of refined parameters	95
GooF	1.146
$(\Delta/\sigma)_{max}$	0.001
$\Delta\rho_{min}$, $\Delta\rho_{max}$ (e/Å^3)	-0.81, 0.75

Note: scattering factors for neutral atoms were employed in the refinement.

* performed by scaling process of Nonius program suite DENZO-SMN.

** $w = 1/[\sigma^2(F_o^2) + (0.02P)^2 + 0.4P]$; P = ([max of (0 or F_o^2)] + $2F_c^2$)/3.

Two selected crystal fragments were investigated with a Nonius KappaCCD diffractometer equipped with a 300 µm diameter capillary-optics collimator. Preliminary investigations evidenced a high crystal quality and a primitive trigonal unit cell very similar to that reported by Mandarino *et al*. (1978). Intensity data were collected from one fragment, with a redundancy factor of 3.4 (see Table 1 for details). The measured intensity data were processed with the Nonius program suite DENZO-SMN and corrected for the Lorentz and polarisation effects. Neither superstructure reflections nor other anomalies were seen on the recorded frames. *E*-

Table 2. Fractional atomic coordinates and displacement parameters (x 10^4) for satterlyite.

Atom	*x*	*y*	*z*	U_{eq}/U_{iso}	U_{11}	U_{22}	U_{33}	U_{23}	U_{13}	U_{12}
P(1)	0	0	0.27825(19)	74.5(1.5)	69(2)	U_{11}	85(3)	0	U_{23}	$0.5U_{11}$
P(2)	1/3	2/3	0.52733(14)	67.1(1.2)	74.4(1.7)	U_{11}	52(3)	0	U_{23}	$0.5U_{11}$
P(3)	0.34138(5)	*x*	0.97775(11)	67.6(1.0)	68.6(1.5)	U_{11}	68(2)	-7.4(1.3)	-7.4(1.3)	36.2(1.5)
M(1)	0.32918(3)	0.85077(3)	1.01101(4)	103.2(0.7)	80.7(1.0)	103.8(1.0)	91.6(1.1)	-22.9(0.8)	5.9(0.7)	21.1(0.8)
M(1)	0.17508(3)	0.85376(3)	0.50440(5)	87.0(0.7)	89.8(1.1)	79.0(1.1)	90.9(1.2)	3.8(0.8)	-0.1(0.8)	41.3(0.9)
O(1)	0.87239(16)	*x*	0.3697(5)	192(4)	90(5)	U_{11}	377(11)	58(6)	U_{23}	29(5)
O(2)	0.27631(13)	0.75462(13)	0.6355(3)	120.7(1.9)	152(5)	130(4)	126(4)	-13(4)	-10(4)	105(4)
O(3)	0.26833(16)	*x*	0.7203(3)	119(3)	137(5)	U_{11}	118(6)	-53(4)	U_{23}	96(5)
O(4)	0.12718(12)	0.75025(12)	0.1427(2)	120(2)	85(4)	150(5)	94(4)	-16(4)	-18(3)	35(4)
O(5)	0.47330(15)	*x*	0.9051(4)	134(3)	95(4)	U_{11}	170(8)	4(4)	U_{23}	15(5)
O(6)	1/3	2/3	0.0162(4)	162(4)	213(7)	U_{11}	60(7)	0	U_{23}	$0.5U_{11}$
O(H1)	0.62619(16)	*x*	0.3250(3)	112(3)	121(4)	U_{11}	82(5)	-2(4)	U_{23}	52(5)
O(H2)	0.72336(15)	*x*	0.8162(3)	116(3)	127(5)	U_{11}	100(6)	-28(4)	U_{23}	69(5)
O(H3)	0	0	-0.0305(8)	397(12)	549(19)	U_{11}	95(15)	0	U_{23}	$0.5U_{11}$
H(1)	0.563(4)	*x*	0.416(10)	240(110)	-	-	-	-	-	-
H(2)	0.805(4)	*x*	0.904(9)	210(110)	-	-	-	-	-	-

Note: Refined occupancies for *M* sites are: *M*(1) = ($Fe_{0.838(2)}Mg_{0.162(2)}$) and *M*(2) = ($Fe_{0.706(2)}Mg_{0.294(2)}$). H(1) and H(2) might not be fully occupied; a third, strongly disordered H atom, H(3), could not be refined, but its average position appears to be close to (0, 0, -0.20) (see text and Fig. 2).

Table 3. Selected interatomic distances (Å) in satterlyite.

M(1)–O(5)	2.0942(13)	P(1)–O(1) x3	1.5205(19)
–O(4)	2.0943(12)	–O(H3)	1.556(4)
–O(2)	2.1157(14)	<P(1)–O>	1.529
–O(H1)	2.1847(12)	P(2)–O(2) x3	1.5364(12)
–O(H2)	2.2808(14)	–O(6)	1.555(2)
–O(6)	2.3593(10)	<P(2)–O>	1.541
<*M*(1)–O>	2.188	P(3)–O(4) x2	1.5350(12)
M(2)–O(3)	2.0740(10)	–O(3)	1.5399(17)
–O(2)	2.0783(12)	–O(5)	1.5421(19)
–O(4)	2.0880(12)	<P(3)–O>	1.538
–O(1)	2.0985(14)	O(H1)–H(1)	0.85(5)
–O(H2)	2.1543(13)	O(H2)–H(2)	1.02(5)
–O(H1)	2.2180(14)		
<*M*(1)–O>	2.119		

Table 4. Bond-valence analysis for satterlyite.

	M(1)	*M*(2)	P(1)	P(2)	P(3)	Sum*
O(1)	-	0.36 x2	1.25 ↓x3	-	-	1.98
O(2)	0.35	0.38	-	1.20 ↓x3	-	1.94
O(3)	-	0.39 x2	-	-	1.19	1.96
O(4)	0.37	0.37	-	-	1.21 ↓x2	1.95
O(5)	0.37 x2	-	-	-	1.18	1.93
O(6)	0.18 x3	-	-	1.14	-	1.69
O(H1)	0.29	0.26	-	-	-	1.11
O(H2)	0.22 x2	0.31 x2	-	-	-	1.07
O(H3)	-	-	1.14	-	-	1.14
Sum*	1.79	2.08	4.89	4.75	4.78	

Note: bond-valence parameters used are from Brese & O'Keeffe (1991).

* Sum values are derived from unrounded bond-valence contributions and their contributions correspond to the refined occupancies (Fe:Mg ratios) of the *M* sites.

statistics indicated an acentric structure and the evaluation of systematic absences showed the space group to be *P*31*m*. The structure was solved by Patterson methods (SHELXS-97, Sheldrick, 1997a) and refined employing SHELXL-97 (Sheldrick, 1997b). The refinement proceeded swiftly and two H atoms could be located on Fourier difference maps. Their positions were refined without any restraints. A third H atom was found which is strongly disordered, and its positional parameters were impossible to refine (see Discussion). An anisotropic treatment of all non-H atoms gave a preliminary discrepancy factor *R*1 = 3.2 %. A subsequent refinement of the Fe:Mg occupancy ratios of the two non-equivalent Fe sites yielded the ratios 0.838(2):0.162(2) and 0.706(2):0.294(2) for the *M*(1) and *M*(2) sites, respectively (the very minor Mn content has been neglected during the calculations). Ultimate refinement cycles gave the final discrepancy factors *R*1 = 2.15 % and w*R*2 = 4.88 %, for 2320 unique reflections with $F_o > 4\sigma(F_o)$ and 95 refined parameters (Table 1). The maximum peaks in the final difference-Fourier maps were -0.81 and 0.75 e/Å^3, respectively. The refined Flack parameter was 0.022(12). The final positional and displacement parameters are given in Table 2, selected bond lengths in Table 3, and a bond-valence analysis is presented in Table 4. A list of observed and calculated structure factors (Table 5) can be obtained from the authors or through the E.J.M. Editorial Office-Paris.

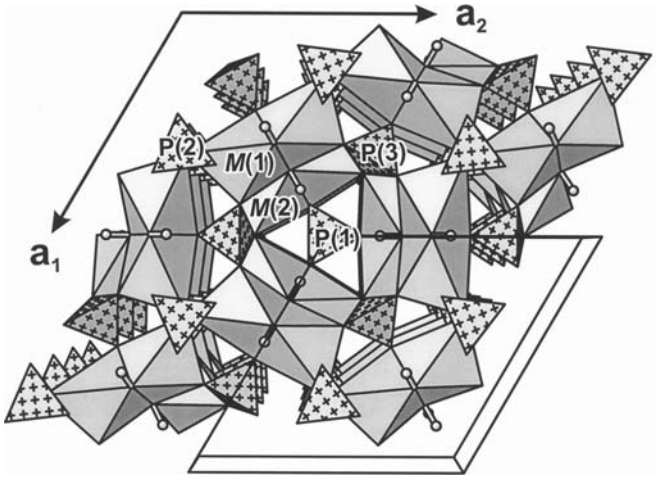

Fig. 1. Perspective view of the satterlyite structure along the *c*-axis (the unit cell is outlined). Pairs of face-sharing $(Fe,Mg)O_6$ octahedra share edges with other octahedra to form double chains running along the *c*-axis. PO_4 tetrahedra are shown with crosses. All drawings were done with ATOMS (v. 5.0, Shape Software 1999).

Description and discussion of the structure

Satterlyite is isostructural with holtedahlite, $Mg_{12}(PO_3OH)(PO_4)_5(OH,O)_6$ (Rømming & Raade, 1989). Like synthetic holtedahlite, the sample studied shows no carbonate-for-phosphate substitution. The presently determined unit-cell parameters of satterlyite, a = 11.355(1), c = 5.0394(5) Å, V = 562.71(9) Å^3, are almost identical to those of the satterlyite type material, a = 11.361, c = 5.041 Å, V = 563.5 Å^3 (Mandarino *et al*., 1978). The excess water content determined by Mandarino *et al*. (1978) and resulting in the empirical formula $(Fe^{2+}_{1.21}Mg_{0.36}Fe^{3+}_{0.19}H_{0.16}Na_{0.10}Mn_{0.04})_{\Sigma 2.06}P_{0.99}Si_{0.01}O_4(OH)$ are in agreement with the present results.

The atomic arrangement in satterlyite is based on three unique PO_4 tetrahedra and two unique, fairly distorted MO_6 octahedra [M = (Fe,Mg)]. Pairs of face-sharing MO_6 octahedra are linked by edge-sharing to form double chains along [001] (Fig. 1). Each double chain shares ligands with six other double chains to produce a three-dimensional network, which hosts the three PO_4 tetrahedra. Corner-linkage provides the connection between PO_4 tetrahedra and MO_6 octahedra. The structure is related to that of phosphoellenbergerite, $Mg_{14}(PO_4)_6(PO_3OH)_2(OH)_6$ (hexagonal, $P6_3mc$), which contains similar double chains of MgO_6 octahedra and PO_4 tetrahedra, but additionally single chains of face-sharing MgO_6 octahedra (Brunet & Schaller, 1996; Raade *et al*., 1998).

The refined occupancies of the M sites, $M(1) = Fe_{0.838(2)}Mg_{0.162(2)}$ and $M(2) = Fe_{0.706(2)}Mg_{0.294(2)}$, correspond to an overall (Fe[+Mn]):Mg ratio of about 3.39, which is close to that of the type material, (Fe+Mn):Mg ~3.46 (Mandarino *et al*., 1978). The average bond-lengths in the two MO_6 octahedra also reflect the preference of the smaller Mg for the second site (<M(1)–O> = 2.188 Å, < M(2)–O> = 2.119 Å). The average M–O distances in satterlyite are longer than those in (natural/synthetic) holtedahlite by 0.055/0.049 Å (M(1) site) and 0.043/0.043 Å (M(2) site). The larger difference for the M(1)-O distances in the two minerals reflects the higher content of the slightly larger Fe^{2+} cations on the M(1) site in the satterlyite structure. The $M(2)O_6$ octahedron in satterlyite is somewhat less distorted than the $M(1)O_6$ octahedron (Table 3). Based on reported average metal–O distances for [6]-coordinated Fe^{2+}, Mg and Mn^{2+} (Baur, 1981), it appears probable that the very minor Mn detected by the chemical analysis is incorporated at the M(1) site. Calculated bond valences of the M sites amount to 1.79 v.u. (valence units) for M(1) and 2.08 v.u. for M(2) (Table 4). The fairly minor Fe^{3+} detected by Mandarino *et al*. (1978; Fe^{2+}:Fe^{3+} ratio 6.42:1.00) will of course influence the bond-valence sums to some small extent (it would lead to a slight increase of the sums), but has been neglected because the Fe^{3+} content in the studied sample is certainly very subordinate – the colour of even relatively large, ~1-mm grains of our sample is pale yellow; any larger Fe^{3+} contents would lead to strong charge-transfer colour effects due to the tight polyhedral linkages. The relatively high Mg contents of the studied sample suggest that, theoretically, an intermediate solid solution member very rich in Mg might exist which could have dominant Fe on the M(1) site, but dominant Mg on the M(2) site.

Phosphate tetrahedra and hydrogen atoms in satterlyite

The $P(3)O_4$ tetrahedron shows a fairly regular geometry, with P–O bond distances of 1.535 (2x), 1.540 and 1.542 Å. By contrast, the other two phosphate tetrahedra, $P(2)O_4$ and $P(1)O_4$, both have three shorter bonds (1.536 x3 and 1.521 x3 Å, respectively) and one longer bond (P(2)–O(6) = 1.555 Å and P(1)–O(H3) = 1.556 Å), therefore suggesting the presence of PO_3OH groups with H atoms bonded to the apical ligands O(6) and O(H3) (*cf*. Ferraris & Ivaldi, 1984). The O(6) atom has as closest anionic neighbours three of the O ligands of the $M(1)O_6$ octahedron at a distance of 2.359 Å, and its calculated bond valence, 1.69 v.u. (valence units), suggests that it is not completely saturated (Table 4). The comparatively large displacement parameters of O(6) in the (001) plane are explained by the long distances to its next neighbours and its need for a higher (local) charge saturation (Table 3). It seems possible that O(6) is bonded to an undetectable disordered H site with a very low occupancy.

The apical O(H3) which is *only* bonded to P(1), is also characterised by comparatively high displacement parameters with a markedly anisotropic behaviour – the ellipsoid is flattened parallel to the (001) plane, as shown in Fig. 2 (see also Table 2). The high degree of freedom of movement of O(H3) is further reflected by the comparatively large standard uncertainty of the P(1)–O(H3) bond distance (Table 3). Because the bond-valence sum of O(H3) only amounts to 1.14 v.u., O(H3) must be bonded to an H atom. A closer inspection of the Fourier difference map at the final state of the refinement had indeed revealed four positive peaks with similar heights at distances to O(H3) between 1.36 and 0.84 Å, indicating that the H(3) atom is present but strongly dis-

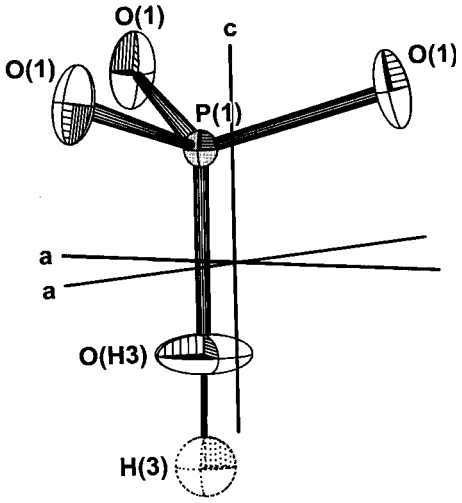

Fig. 2. View of the $P(1)O_4$ tetrahedron showing the strongly vibrating O(H3) and O(1) atoms and the approximate average position of the disordered H(3) atom at (0, 0, –0.20). Displacement ellipsoids are drawn at 50 % probability.

ordered. As already noted above, the (average) position of H(3) was impossible to refine, although it appeared to be near (0, 0, -0.20) (Fig. 2). The variability of the O(H3)-H(3) bond also influences the positional parameters of the three equivalent O(1) atoms, which form the base of the $P(1)O_4$ tetrahedron (Table 3). In fact, all other dominant residual peaks in the difference map were close to O(1) and P(1). The other two detected H atoms, H(1) and H(2), are each bonded to O ligands shared by the two MO_6 octahedra. These H atoms are characterised by normal displacement parameters (Table 2). The distances of the O(H1), O(H2) and O(H3) atoms to possible acceptors of hydrogen bonds are all > 3.2 Å, thus allowing only very weak hydrogen bonding. This neglects, however, the disordered character of H(3) (see also discussion of IR spectra below) and other possible local defects involving H(1) and H(2), and the very minor amounts of Fe^{3+} and Mn.

The three detected H positions would correspond to seven H atoms per formula unit. If these positions were fully occupied, the resulting stoichiometry would contradict the proposed chemical formula of satterlyite, $(Fe^{2+},Mg)_2(PO_4)OH$ (Mandarino *et al*., 1978). Thus, the correct structural formula of the investigated crystal has been written $(Fe,Mg,Mn)_{12}(PO_3OH)(PO_4)_5(OH,O)_6$, with $Z = 1$. The positions of the three H atoms (OH groups) in satterlyite correspond to those reported for synthetic holtedahlite, $Mg_{12}(PO_3OH)(PO_4)_5(OH,O)_6$ (Rømming & Raade, 1989). Partial occupancies of all three OH groups were inferred for holtedahlite. In synthetic holtedahlite only two H atoms, H(1) and H(2), were detectable, whereas the data for natural holtedahlite did not allow the direct location of H sites (Rømming & Raade, 1989). A comparison of the refined displacement parameters of the atoms in holtedahlite and satterlyite demonstrates that the H disorder is considerably less pronounced in the latter. A recent detailed study of the H atoms in synthetic holtedahlite, using infrared spectroscopy and nuclear magnetic resonance (Brunet & Schaller, 1996), confirmed the results of the single-crystal investigations of Rømming & Raade (1989). It is noteworthy that in the structurally related phosphoellenbergerite, $Mg_{14}(PO_4)_6(PO_3OH)_2(OH)_6$, there also exist disordered and only partially occupied H sites (Brunet & Schaller, 1996).

In natural holtedahlite, a CO_3 group partially substitutes for the $P(1)O_4$ group (Rømming & Raade, 1989). In satterlyite, no residual electron density was present at the theoretical C atom position. The most positive peaks in the final Fourier difference map for satterlyite were close to the atoms O(H3), O(1) and P(1), explained by the influence of the disordered H(3) atom on the geometry of the $P(1)O_4$ tetrahedron, as discussed above.

A certain Mg content might be necessary to stabilise the satterlyite structure, although analyses of its 'dimorph' wolfeite, demonstrate that the latter can also contain considerable Mg – the formula $(Fe_{1.65}Mg_{0.20}Mn_{0.15})_2(PO_4)(OH_{0.95}F_{0.05})$ is reported by Robinson *et al*. (1992) for samples from the satterlyite type locality. The packing efficiency V_E values of the two 'dimorphs', defined as the unit cell volume divided by the total number of anions in the respective cells (Moore, 1984), are 18.75 (satterlyite) and 19.02 (wolfeite). Wolfeite is more common at the Canadian locality than satterlyite (Robertson, 1982). Thus, wolfeite may be the more stable compound at the given conditions (low pressure, low temperature). For the Mn^{2+} analogue of wolfeite, triploidite, $(Mn^{2+},Fe^{2+})_2(PO_4)OH$, V_E amounts to 19.38. No trigonal 'dimorph' of triploidite is known at present. The calculated packing efficiencies are similar to those of closest-packed oxides and explain the fairly high hardness (4-5), missing cleavage and conchoidal fracture of these phosphates.

Infrared absorption spectra

The free phosphate ion has T_d symmetry giving rise to four normal modes of vibrations with representation A_1 (ν_1), E (ν_2), and 2 x T_2 (ν_3 and ν_4). All fundamentals are Raman-active, but only the triply degenerated states are IR-active. The fundamental frequencies of a phosphate ion are ν_1= 938, ν_2 = 420, ν_3 = 1017 and ν_4= 567 cm^{-1} (*cf*. Ross, 1974; after Nakamoto, 1970). The IR powder spectrum of satterlyite is given in Figure 3. It shows one broad band system in the spectral range of 1250 to 700 cm^{-1} and a second system from 650 to 500 cm^{-1}. As a first approximation, the high-energy band system is attributed to the fundamentals ν_3 (anti-symmetric stretching mode) and the second band system to the fundamentals ν_4 (bending mode) of the three structurally different phosphate groups (according to T_d symmetry). A detailed assignment of individual bands is not possible because a local T_d point symmetry for the phosphate groups is no longer valid. Thus, the spectrum will become more complicated, giving rise to further energy-level splittings, and components of the fundamentals ν_1 and ν_2 may become IR-active, too. In addition, combination modes and overtones, e.g., $2\nu_2$, $2\nu_4$ and $\nu_2 + \nu_4$ (labelling with respect to T_d symmetry) derived from all phosphate groups will superimpose. The positions of the five discernible maxima in the broad band ranging from 1250 to 700 cm^{-1} (Fig. 3) are very close to those mentioned by Raade & Mladeck (1979), 1115,

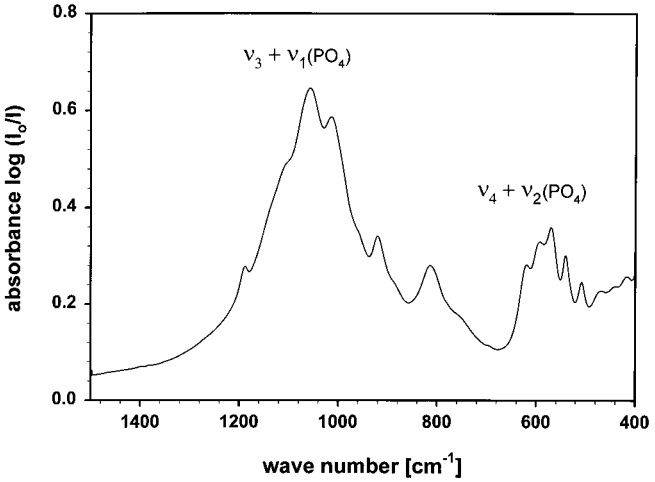

Fig. 3. Infrared powder spectrum of satterlyite in the spectral range of 1500 to 400 cm^{-1}. The spectrum shows only bands caused by PO_4 groups.

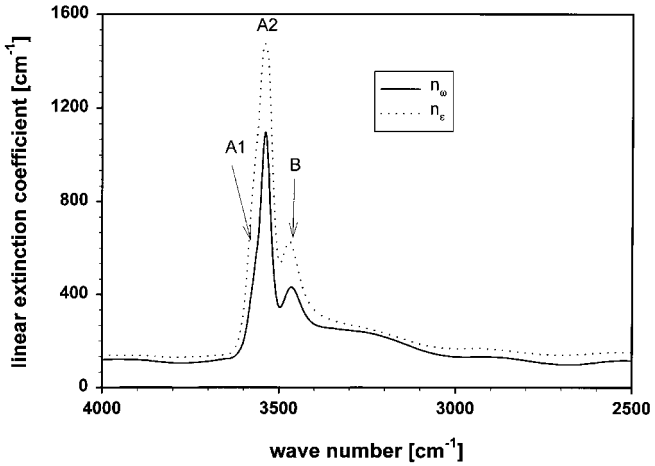

Fig. 4. Polarised infrared spectra of a satterlyite single crystal parallel and perpendicular to [001] in the O-H stretching vibrational region.

1045, 1010, 920 and 815 cm^{-1}. The powder spectrum gives no evidence for the presence of any carbonate groups in the mineral, in agreement with the conclusions of Raade & Mladeck (1979) and Rømming & Raade (1989).

Polarised single-crystal infrared spectra in the O-H stretching vibrational region recorded parallel to n_ω and n_ε are presented in Figure 4. The hydroxyl bands show a pleochroic behaviour with the highest intensity parallel to n_ε. The spectra are very similar to those of holtedahlite (Brunet & Schaller, 1996). Each spectrum consists of a strong band (A2) at 3536 cm^{-1} which exhibits a weak shoulder (A1) at ~3568 cm^{-1}, and a second medium-strong, asymmetric band (B) at 3471 cm^{-1} (Table 6). By analogy to holtedahlite the higher-energy bands A1 and A2 are assigned to the O-H stretching vibrations of OH(1) and OH(2), since the protons are in a very similar atomic environment attached to the double chains. Band B is assigned to the stretching vibration of the OH(3) group of the partly protonated P(1)O_4 group.

Table 6. Infra-red absorption bands (cm^{-1}) in the O-H stretching vibrational region of satterlyite compared to literature data and data for holtedahlite.

	Satterlyite		Holtedahlite	
	This work	Raade & Mladeck (1979)	Brunet & Schaller (1996)	Raade & Mladeck (1979)
O(H1)-H(1) & O(H2)-H(2)	3536, ~3568 (sh)	3540	3567 (fs)	3565
O(H3)-H(3)	3471	–	3472	– *

Note: sh = shoulder, fs = band with fine structure.
* A small bump at roughly 3400 cm^{-1} is, however, recognisable in the published spectrum.

The higher band intensity parallel to n_ε is consistent with the orientation of the OH(3)-H(3) vector approximately parallel to the *c*-axis. The difference in band intensity for the A1 and A2 bands is lower because the corresponding O-H vectors have components along both principal crystallographic axes (Fig. 1). The corresponding first overtones of the O-H stretching vibrations are observed at 7075 cm^{-1} ($2\nu_{A2}$), 7151 cm^{-1} ($2\nu_{A1}$) and 6938 cm^{-1} ($2\nu_B$), respectively. Using the correlation of O-H stretching frequencies and O-H···O hydrogen bond lengths in minerals by Libowitzky (1999), the observed O-H stretching frequencies in satterlyite, ~3568, 3536 and 3471 cm^{-1}, would correspond to approximate O···O bond lengths of 3.10, 3.05 and 2.90 Å, respectively. The two longer distances are in reasonable agreement with the results of the structure solution, considering the strong scatter of the correlation curve in this region (Libowitzky, 1999). The asymmetric broad band at 3471 cm^{-1} indicates variable O-H and O···O distances, in agreement with a disordered and partially occupied H(3) site. A comparison with published infrared spectra of holtedahlite (Raade & Mladeck, 1979; Brunet & Schaller, 1996) in Table 6 demonstrates that the substitution of Fe^{2+} for Mg leads to only very small shifts of the stretching frequencies of OH(1) and OH(2).

Thermogravimetric data

The thermogravimetric curve, from which a blank run was subtracted, shows several features: a weight loss starts at 463°C, is followed by a small step at 473°C (possibly an artefact due to grain size distributions or other effects) and continues until 550°C. Thereafter, a weight gain is observed which levels out at about 770°C and remains more or less constant until an additional weight loss starts at approximately 860°C. The first weight loss is attributed to the loss of water, possibly in two or more steps. The subsequent weight gain is caused by the oxidation of Fe^{2+} (and the very subordinate amounts of Mn) which is unavoidable despite the use of high-purity nitrogen gas, and is also expected by comparison with the oxidation behaviour of other hydrated Fe^{2+} phosphates. The weight gain overlaps the first weight loss and unfortunately makes a determination of the total loss of water impossible – the maximum weight loss at the

starting point of the oxidation was only 0.66 %. The brown-red oxidation product was found by X-ray powder diffraction to be a mixture of hematite and at least one unidentified compound. The thermogravimetric data are comparable to those obtained by Mandarino *et al*. (1978) using an oxygen atmosphere (heating rate not given but probably higher than 1 K/min). They observed a weight loss beginning at a higher temperature (about 531 °C) and continuing to about 603 °C, after which a weight gain ensued and continued to about 943°C.

Acknowledgements: Dr. Y. Le Page is especially thanked for encouraging us to publish the present results. A. Wagner kindly prepared the thin sections. Dr. E. Libowitzky and Dr. G. Raade provided valuable comments on the manuscript. Constructive reviews by Dr. F. Brunet, Dr. G. Cruciani and Prof. C. Chopin further improved the text.

References

Baur, W.H. (1981): Interatomic distance predictions for computer simulation of crystal structures. *in* "Structure and bonding in crystals", Vol. **II**, O'Keeffe, M. & Navrotsky, A., eds., Academic Press, New York, Chapter 15, 31-52.

Brese, N.E. & O'Keeffe, M. (1991): Bond-valence parameters for solids. *Acta Cryst.*, **B47**, 192-197.

Britvin, S.N., Pakhomovskii, Ya.A., Bogdanova, A.N. (1996): Krasnovite, $Ba(Al,Mg)(PO_4,CO_3)(OH)_2 \cdot H_2O$ – a new mineral. *Zap. Vses. Mineral. Obshch*., **125**, 110-12.

Brunet, F. & Schaller, T. (1996): Protons in the magnesium phosphates phosphoellenbergerite and holtedahlite; an IR and NMR study. *Am. Mineral*., **81**, 385-394.

Comodi, P. & Liu, Y. (2000): CO_3 substitution in apatite: further insight from new crystal-chemical data of Kasekere (Uganda) apatite. *Eur. J. Mineral*., **12**, 965-974.

Ferraris, G. & Ivaldi, G. (1984): *X*-OH and O-H...O bond lengths in protonated oxyanions. *Acta Cryst*., **B40**, 1-6.

Frondel, C. (1949): Wolfeite, xanthoxenite, and whitlockite from the Palermo mine, New Hampshire. *Am. Mineral*., **34**, 692-705.

Griffiths, P.R. & de Haseth, J.A. (1986): Fourier transform infrared spectroscopy (Chemical Analysis, Vol. **83**). Wiley, New York.

Libowitzky, E. (1999): Correlation of O-H stretching frequencies and O-H···O hydrogen bond lengths in minerals. *Mh. Chemie*, **130**, 1047-1059.

Mandarino, J.A., Sturman, B.D., Corlett, M.I. (1978): Satterlyite, a new hydroxyl-bearing ferrous phosphate from the Big Fish River area, Yukon Territory. *Can. Mineral*., **16**, 411-413.

Mertz, L. (1965): Transformation in Optics. Wiley, New York.

Moore, P.B. (1984): Crystallochemical aspects of the phosphate minerals. *in* "Phosphate minerals", J.O. Nriagu & P.B. Moore, eds., Springer Verlag, Berlin, 155-170.

Nakamoto, K. (1970): Infrared spectra of inorganic and coordination compounds. 2nd ed., Wiley, New York.

Raade, G. & Mladeck, M.H. (1979): Holtedahlite, a new magnesium phosphate from Modum, Norway. *Lithos*, **12**, 283-287.

Raade, G., Rømming, C., Medenbach, O. (1998): Carbonate-substituted phosphoellenbergerite from Modum, Norway: description and crystal structure. *Mineral. Petrol.*, **62**, 89-101.

Regnier, P., Lasaga, A.C., Berner, R.A., Han, O.H., Zilm, K.W. (1994): Mechanism of CO_3^{2-} substitution in carbonate-fluorapatite: Evidence from FTIR spectroscopy, ^{13}C NMR, and quantum mechanical calculations. *Am. Mineral*., **79**, 809-818.

Robertson, B.T. (1982): Occurrence of epigenetic phosphate minerals in a phosphatic iron-formation, Yukon Territory. *Can. Mineral*., **20**, 177-187.

Robinson, G.W., Van Velthuizen, J., Ansell, H.G., Sturman, B.D. (1992): Mineralogy of the Rapid Creek and Big Fish area Yukon Territory. *Mineral. Rec*., **23**, 4-47.

Rømming, C. & Raade, G. (1989): The crystal structure of natural and synthetic holtedahlite. *Mineral. Petrol*., **40**, 91-100.

Ross, S.D. (1974): Phosphates and other oxy-anions of group V. *in* "The infrared spectra of minerals", Farmer, V.C., ed., Mineral. Soc. Monogr. 4, Mineral. Society, London, 383-422.

Sheldrick, G.M. (1997a): SHELXS-97, a program for the solution of crystal structures. University of Göttingen, Germany.

– (1997b): SHELXL-97, a program for crystal structure refinement. University of Göttingen, Germany.

Received 10 May 2000
Modified version received 15 September 2000
Accepted 8 June 2001